Supporting Information:

Mechanism of Adsorption Affinity and Capacity of $Mg(OH)_2$ to Uranyl Revealed by Molecular Dynamics Simulation

Xinwen Ou,[a,b,e] Zanyong Zhuang,[a] Jingyuan Li,*[,b] Feng Huang[c] and Zhang Lin*[,a,d]

[a] Key Laboratory of Design and Assembly of Functional Nanostructures, Fujian Institute of Research on the Structure of Matter, Chinese Academy of Sciences, Fuzhou, Fujian 350002, China

[b] CAS Key Laboratory for Biomedical Effects of Nanomaterials and Nanosafety, Institute of High Energy Physics, Chinese Academy of Sciences, Yuquan Road 19B, Beijing 100049, China

[c] State Key Laboratory of Optoelectronic Materials and Technologies, School of Physics and Engineering, Sun Yat-Sen University, Guangzhou 510275, China

[d] School of Environment and Energy, South China University of Technology, Guangzhou 510006, China

[e] University of Chinese Academy of Sciences, Beijing 100049, P. R. China

Corresponding Author

*JY Li. Phone: 86-10-88236990; Fax: 86-10-88233191; e-mail: lijingyuan@ihep.ac.cn.

*Z Lin. Fax: 86-591-83705474; e-mail: zlin@fjirsm.ac.cn.

1. Description of force field model and parameters

Potential energy was calculated in Gromacs (v.4.6.5) as the sum of non-bonded (electrostatic and van der Waals) and bonded (bond stretch and bend) interactions. The energy expressions are described by:

$$E = \sum_{bonds} \frac{k_1}{2}(r - r_0)^2 + \sum_{angles} \frac{k_2}{2}(\theta - \theta_0)^2 + \sum_{i<j} \left\{ 4\varepsilon_{ij} \left[\left(\frac{\sigma_{ij}}{r_{ij}} \right)^{12} - \left(\frac{\sigma_{ij}}{r_{ij}} \right)^{6} \right] + \frac{q_i q_j}{4\pi\varepsilon_0 r_{ij}} \right\} \quad (1)$$

Force field parameters of CLAYFF for $Mg(OH)_2$, sodium and chloride ions,[1] flexible SPC for water,[2,3] and parameters for uranyl[4] and carbonate[5,6] were converted for units used in Gromacs (Table S1).

Table S1. Potential parameters

atom type[a]	description	q (e)	σ (nm)	ε (kJ/mol)	source
Mg	hydroxide magnesium	1.050	0.526432	3.77807×10^{-6}	1
Om	hydroxyl oxygen	-0.950	0.316554	0.650194	1
Hm	hydroxyl hydrogen	0.425	0.000	0.000	1
Ow	water oxygen	-0.820	0.316554	0.650194	2,3
Hw	water hydrogen	0.410	0.000	0.000	2,3
U	uranyl uranium	3.250	0.28509	0.50208	4
Ou	uranyl oxygen	-0.625	0.31182	0.83680	4
C	carbonate carbon	0.430	0.38754	0.16319	5,6
Oc	carbonate oxygen	-0.810	0.28598	0.95405	5,6
Cl	chloridion	-1.000	0.439997	0.418818	1
Na	sodion	1.000	0.235001	0.544338	1
bond		k_1 (kJ/mol/nm^2)		r_0 (nm)	
Om-Hm		463700.100		0.100	
Ow-Hw		463700.100		0.100	
U-Ou		418400.000		0.180	
C-Oc		1097881.60		0.1250	
Angle		k_2 (kJ/mol/rad^2)		θ_0 (°)	
Hw-Ow-Hw		383.000		109.47	
Ou-U-Ou		1255.200		180.00	
Oc-C-Oc		12552.000		120.00	

a. The arithmetic mean rule and geometric mean rule are used to the combination of σ and ϵ, respectively.

2. Figures

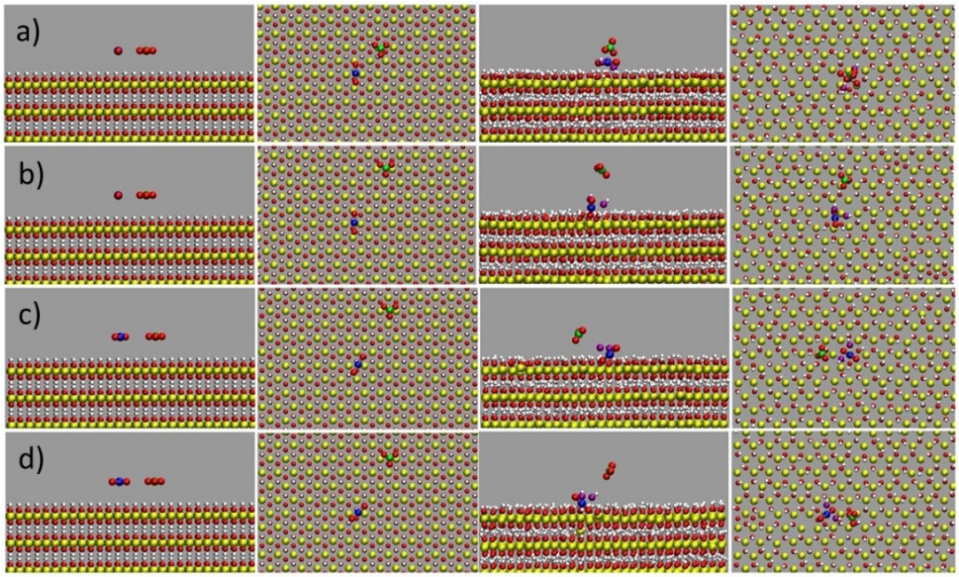

Figure. S1 The initial configurations (orthographic view, top view) and the stable adsorption configurations (orthographic view, top view) for (a) system II, (b) system III, (c) system IV and (d) system V.

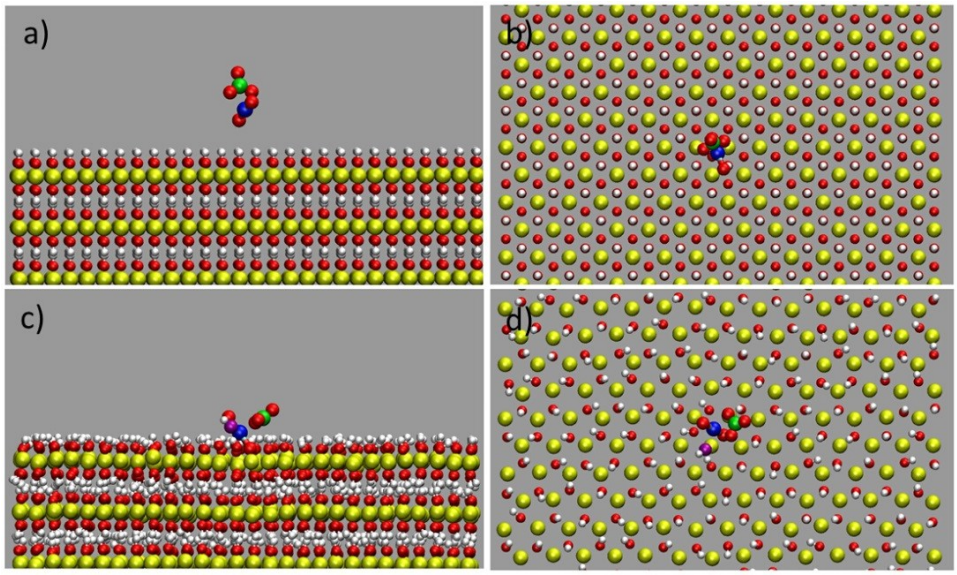

Figure. S2 Uranyl-carbonate-pair system: (a) Orthographic view and (b) top view for the initial configuration. (c) Orthographic view and (d) top view for the stable adsorption configuration.

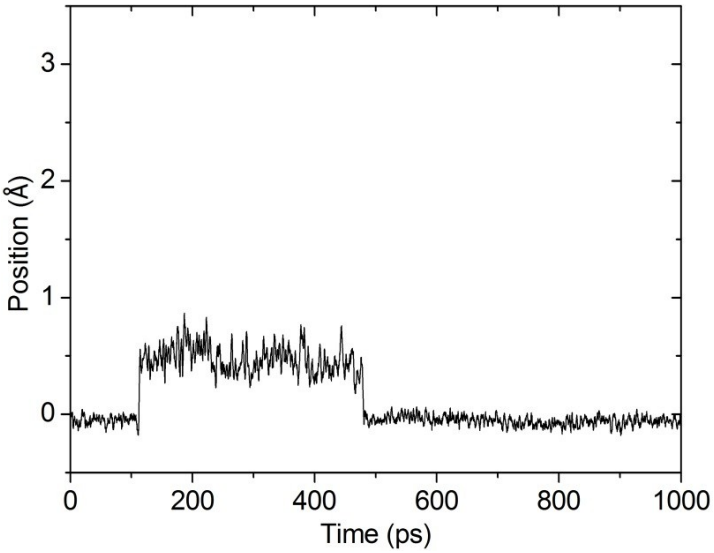

Figure. S3 Time evolution of the position of one adjacent surface OH group.

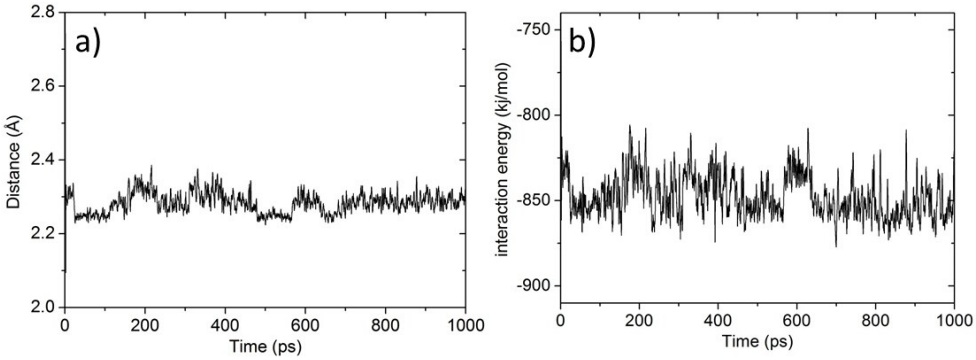

Figure. S4 Time evolution of (a) the distance and (b) the interaction energy between the adsorbed

uranyl cation and the fluctuating OH group.

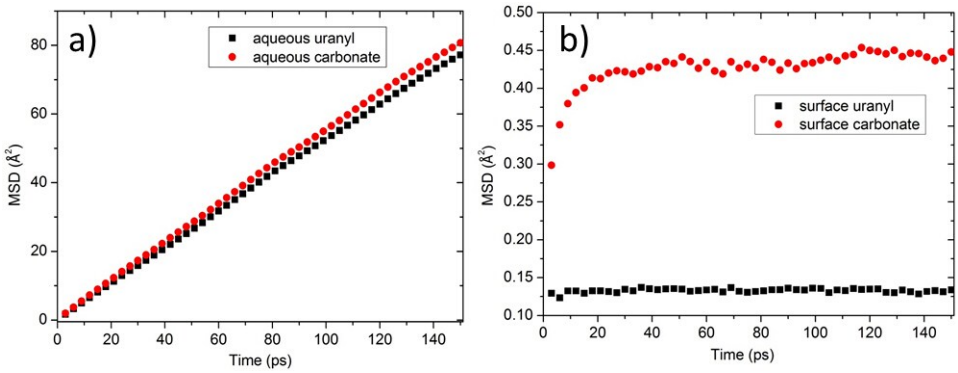

Figure. S5 The mean square displacements for (a) aqueous uranyl and carbonate ions as well as (b) adsorbed uranyl and carbonate ions.

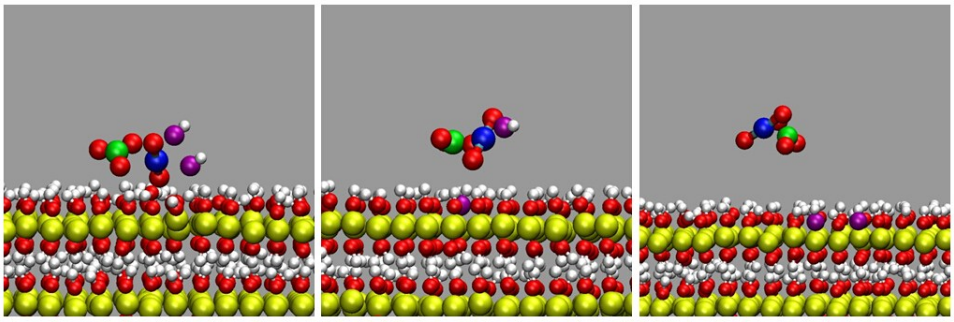

Figure. S6 Representative Snapshots for uranyl at z = 2.72, 4.13, 7.02 Å (from left to right), corresponding to three intermediate states in the free energy profile of uranyl desorption.

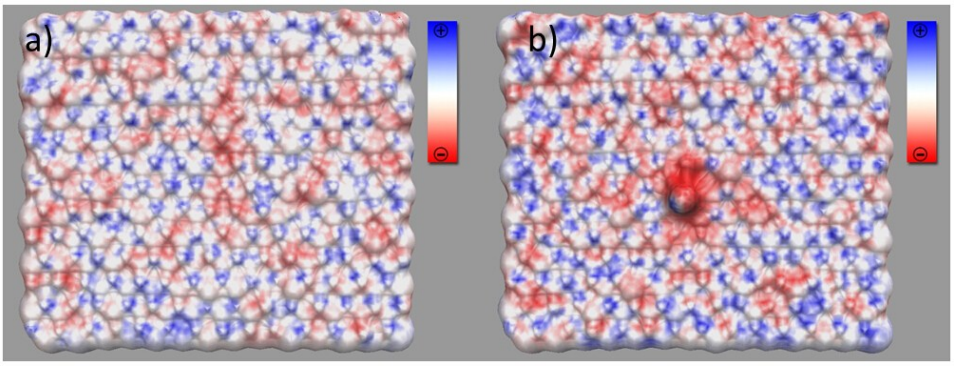

Figure. S7 Uranyl-carbonate-pair system: The electrostatic potentials for the $Mg(OH)_2$ (001) surface (a) before and (b) after the uranyl adsorption, calculated via the APBS software.

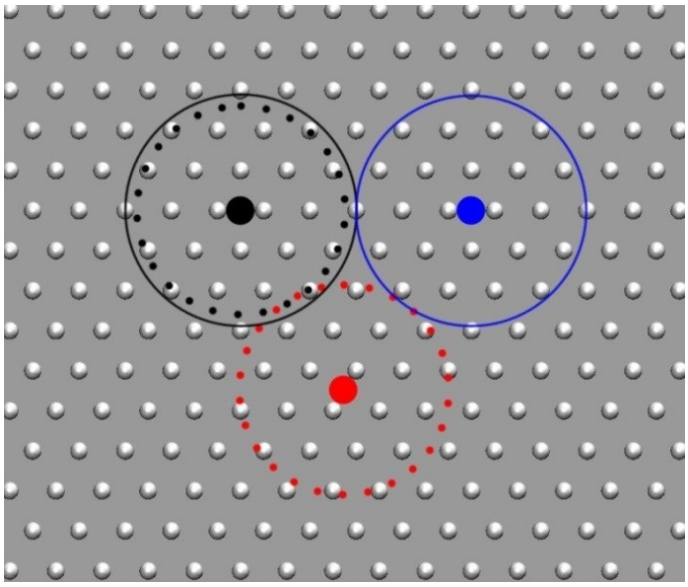

Figure. S8 The schematic diagram for the susceptible region of adsorbed uranyl (black) and two surface distributions of uranyl. The adsorbed uranyl has a profound effect on the orientation of surface OH groups within d_{xy} = 7.1 Å (dotted circle), and a modest effect on the OH groups in the region between d_{xy} = 7.1 Å and d_{xy} = 7.9 Å (solid circle). In the first distribution, modestly affected OH groups are not shared by the adjacent uranyl (blue), while in the second distribution the uranyl (red) share these OH groups. The corresponding distance between adjacent uranyl should be 15.8 Å and 14.2 Å, and the estimated surface density of adsorbed uranyl is then 0.47 nm^{-2} and 0.58 nm^{-2} respectively.

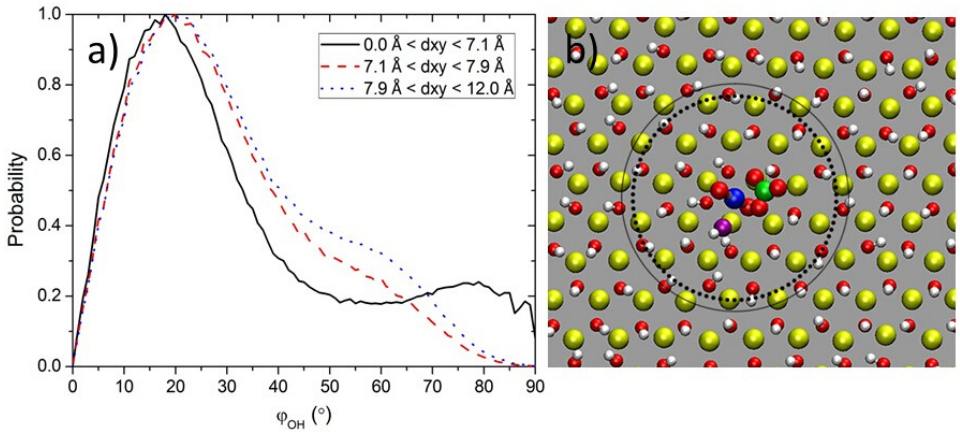

Figure. S9 Uranyl-carbonate-pair system: (a) Distributions of dipole orientation of surface OH groups, φ_{OH}, with different in-plane separation (d_{xy}) from the adsorbed uranyl. (b) The scheme for the susceptible regions of the adsorbed uranyl (d_{xy} = 7.9 Å, solid circle; d_{xy} = 7.1 Å, dotted circle).

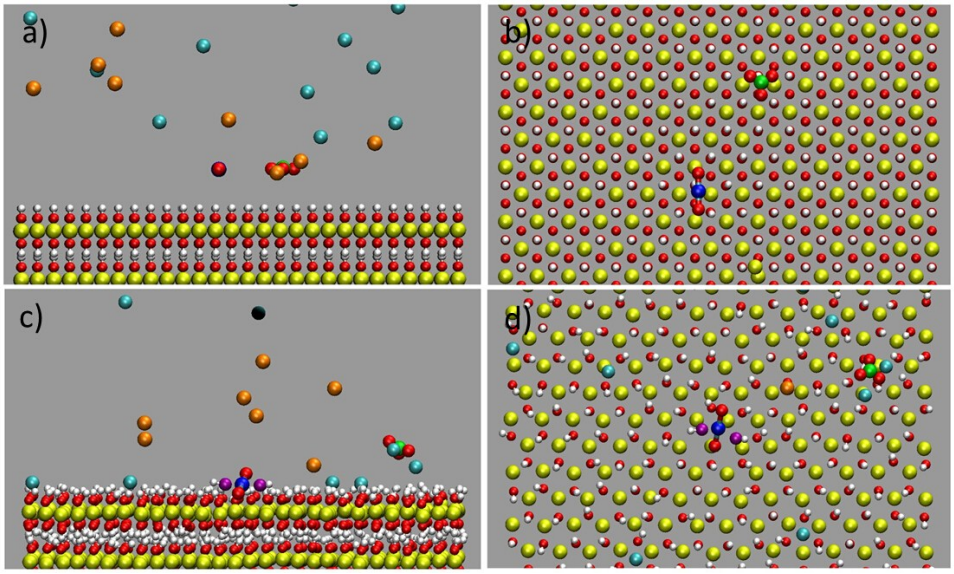

Figure. S10 0.6 M NaCl system: (a) Orthographic view and (b) top view for the initial configuration. (c) Orthographic view and (d) top view for the stable adsorption configuration. The Na and Cl atoms are colored in cyan and orange, respectively.

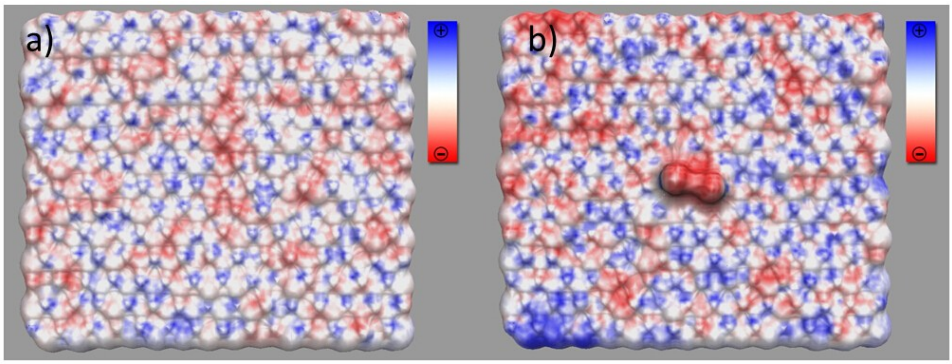

Figure. S11 0.6 M NaCl system: The electrostatic potentials for the $Mg(OH)_2$ (001) surface (a) before and (b) after the uranyl adsorption, calculated via the APBS software.

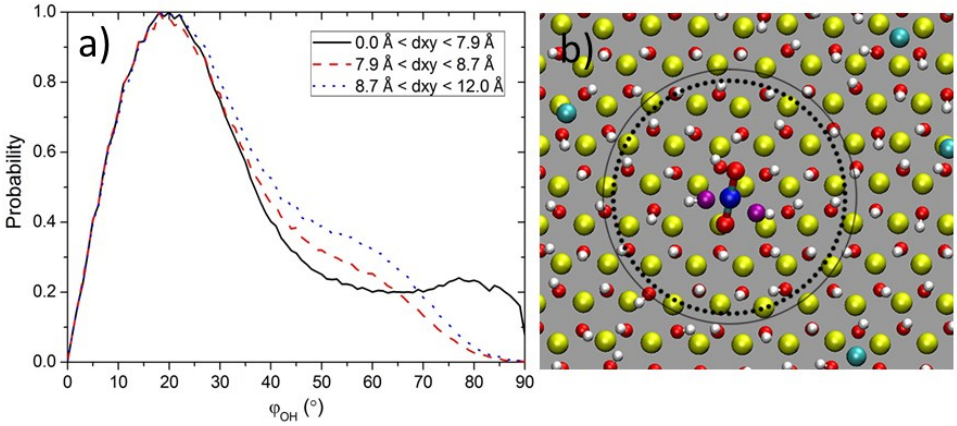

Figure. S12 0.6 M NaCl system: (a) Distributions of dipole orientation of surface OH groups, φ_{OH}, with different in-plane separation (d_{xy}) from the adsorbed uranyl. (b) The scheme for the susceptible regions of the adsorbed uranyl (d_{xy} = 8.7 Å, solid circle; d_{xy} = 7.9 Å, dotted circle).

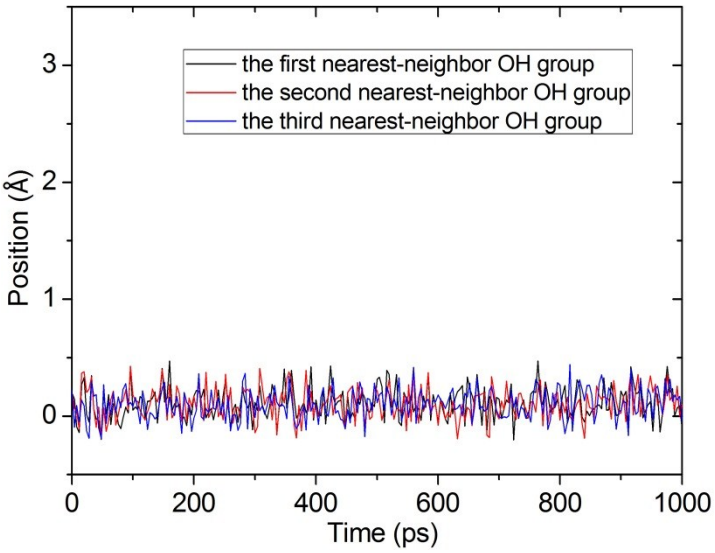

Figure. S13 Time evolution of the positions of three nearest-neighbor OH groups around the adsorbed sodium ion.

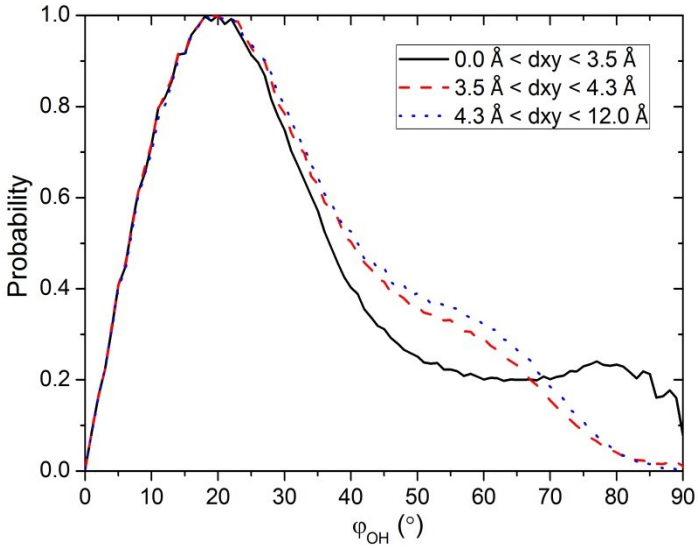

Figure. S14 Distributions of dipole orientation of surface OH groups, φ_{OH}, with different in-plane separation (d_{xy}) from the adsorbed sodium ion.

References

(1) Cygan, R. T.; Liang, J. J.; Kalinichev, A. G., Molecular models of hydroxide, oxyhydroxide, and clay phases and the development of a general force field. *J. Phys. Chem. B* **2004**, *108*, 1255-1266.

(2) Berendsen, H. J. C.; Postma, J. P. M.; Gunsteren, W. F.; Hermans, J. Interaction Models for Water in Relation to Protein Hydration In *Intermolecular Forces*; Pullman, B., Ed.; D. Reidel: Amsterdam, 1981; Vol. 14, pp 331-342.

(3) Teleman, O.; Jönsson, B.; Engström, S., A molecular dynamics simulation of a water model with intramolecular degrees of freedom. *Mol. Phys.* **1987**, *60*, 193-203.

(4) Kerisit, S.; Liu, C., Structure, kinetics, and thermodynamics of the aqueous uranyl(VI) cation. *J. Phys. Chem. A* **2013**, *117*, 6421-6432.
(5) Greathouse, J. A.; O'Brien, R. J.; Bemis, G.; Pabalan, R. T., Molecular Dynamics Study of Aqueous Uranyl Interactions with Quartz (010). *J. Phys. Chem. B* **2002**, *106*, 1646-1655.
(6) Greathouse, J. A.; Cygan, R. T., Molecular dynamics simulation of uranyl(VI) adsorption equilibria onto an external montmorillonite surface. *Phys. Chem. Chem. Phys.* **2005**, *7*, 3580-3586.